Published in final edited form as:
Biomacromolecules. 2012 July 9; 13(7): 2003–2012. doi:10.1021/bm300752j.

Crosslinking and degradation of step-growth hydrogels formed by thiol-ene photo-click chemistry

Han Shih and **Chien-Chi Lin***
Department of Biomedical Engineering, Purdue School of Engineering and Technology, Indiana University - Purdue University at Indianapolis, Indianapolis, IN46202, USA

Abstract

Thiol-ene photo-click hydrogels have been used for a variety of tissue engineering and controlled release applications. In this step-growth photopolymerization scheme, multi-arm poly(ethylene glycol) norbornene (PEG4NB) was crosslinked with di-thiol containing crosslinkers to form chemically crosslinked hydrogels. While the mechanism of thiol-ene gelation was well described in the literature, its network ideality and degradation behaviors are not well-characterized. Here, we compared the network crosslinking of thiol-ene hydrogels to Michael-type addition hydrogels and found thiol-ene hydrogels formed with faster gel points and higher degree of crosslinking. However, thiol-ene hydrogels still contained significant network non-ideality, demonstrated by a high dependency of hydrogel swelling on macromer contents. In addition, the presence of ester bonds within the PEG-norbornene macromer rendered thiol-ene hydrogels hydrolytically degradable. Through validating model predictions with experimental results, we found that the hydrolytic degradation of thiol-ene hydrogels was not only governed by ester bond hydrolysis, but also affected by the degree of network crosslinking. In an attempt to manipulate network crosslinking and degradation of thiol-ene hydrogels, we incorporated peptide crosslinkers with different sequences and characterized the hydrolytic degradation of these PEG-peptide hydrogels. In addition, we incorporated a chymotrypsin-sensitive peptide as part of the crosslinkers to tune the mode of gel degradation from bulk degradation to surface erosion.

Keywords

Thiol-ene chemistry; hydrogel; photopolymerization; degradation

Introduction

An ongoing effort in biomaterial science and engineering is to design hydrogels with tunable and predictable degradation behaviors, because degradable hydrogels are particularly useful as provisional matrices for tissue regeneration and as carriers for controlled protein delivery.[1-4] Among all degradation mechanisms, hydrolytic degradation of synthetic hydrogels has received significant attention due to the simplicity of hydrolysis mechanism

*To whom correspondence should be addressed: lincc@iupui.edu Chien-Chi Lin, Ph.D., Assistant Professor, Department of Biomedical Engineering, Indiana University-Purdue University at Indianapolis, Indianapolis, IN 46202, Phone: 317-274-0760, Fax: 317-278-2455.

and well-defined polymer chemistry.[5-7] A classical way of preparing hydrolytically degradable hydrogels is by chain-growth photopolymerization of acrylated macromers, such as terminally acrylated poly(lactic acid)-*b*-poly(ethylene glycol)-*b*-poly(lactic acid) (acryl-PLA-*b*-PEG-*b*-PLA-acryl) tri-block copolymers.[5, 8] The hydrolytic degradation rate of these hydrogels could be tuned and predicted by using copolymers with different lengths of lactide repeating units.[6, 7] Similarly, other hydrolytically labile ester bonds could be incorporated to the termini of PEG macromers prior to acrylation or methacrylation.[9, 10]

In addition to the chain-growth polymerized hydrogels, step-growth polymerized gels could also be rendered hydrolytically degradable. For example, Hubbell and co-workers developed Michael-type addition hydrogels through nucleophilic reactions between acrylates on multi-arm PEG macromer and sulfhydryl groups on the crosslinkers.[11, 12] Thioether-ester linkages formed between acrylate and sulfhydryl moieties were hydrolytically labile and the degradation rates of these hydrogels could be tuned by controlling macromer concentration and functionality.[11, 13, 14] Bowman and colleagues performed experimental and theoretical investigations on hydrolytic degradation of step-growth thiol-acrylate and thiol-allylether photopolymers.[15-18] Degradation was readily tuned and predicted using monomers with different concentration, functionality, and degradability. More recently, Leach and colleagues developed hydrolytically degradable Michael-type hydrogels based on 4-arm PEG-vinylsulfone (PEGVS) and PEG-diester-dithiol.[19, 20] Degradation of these step-growth hydrogels was altered by tuning the number of methylene groups between the thiol and ester moieties in the PEG-diester-dithiol linkers.

While these degradable hydrogels have found various successful applications, limitations and challenges exist. For instance, chain-growth photopolymerized hydrogels are known to form dense hydrophobic polyacrylate chains[21] that yield network heterogeneity and high molecular weight degradation products.[5-7] On the other hand, the formation of step-growth Michael-type hydrogels often requires long gelation time that leads to the formation of high degrees of network defects.[13] It has been shown that high macromer functionalities (e.g., 8-arm PEG-acrylate) and concentrations (e.g., >50 wt%) were necessary for step-growth Michael-type addition hydrogels to approach an ‘ideal’ network structure.[13]

To overcome the disadvantages facing hydrogels formed by chain-growth photopolymerizations and step-growth Michael-type addition reactions, Anseth and colleagues recently introduced a new class of PEG-peptide hydrogels based on radical-mediated orthogonal thiol-ene photo-click reaction.[22] In this system, low intensity and long wavelength (5 – 10 mW/cm^2, 365 nm) ultraviolet light was used to generate thiyl radicals (from bis-cysteine-containing oligopeptides), which crosslinked with ene moieties on norbornene-functionalized 4-arm PEG (PEG4NB) to form a step-growth network. This reaction scheme preserves all advantages offered by photopolymerizations, including rapid, ambient, and aqueous reaction conditions, as well as spatial-temporal control over gelation kinetics. Step-growth thiol-ene photo-click reactions are not oxygen inhibited,[23] thus yielding more rapid gelation kinetics compared to chain-growth photopolymerizations.[24] Comparing to step-growth Michael-type gelation, thiol-ene photo-click reactions have reduced disulfide bond formation due to radical-mediated cleavage,[25] thus increasing the extent of crosslinking that results in higher mechanical properties at similar macromer

contents.[22] Furthermore, the orthogonal and step-growth nature of norbornene-sulfhydryl reaction permits dynamic modification of hydrogel biochemical and biophysical properties in the presence of cells.[22] Several cell types have been encapsulated successfully by these PEG-peptide hydrogels, including human mesenchymal stem cells,[26] fibroblasts,[22, 27] fibrosarcoma,[27] valvular insterstitial cells,[28] and radical-sensitive pancreatic β-cells.[24] Enzymatically degradable peptides could also be utilized to crosslink thiol-ene hydrogels for enzyme-responsive controlled release applications.[29]

While thiol-ene photopolymerized hydrogels have emerged as an attractive class of biomaterials, the structure-property relationships of these hydrogels have not been extensively characterized. For example, an 'ideal network' was often mentioned in previous publications even with the use of low macromer concentrations (2 wt% to 10 wt% of PEG4NB) and no detailed characterization of hydrogel network properties was performed.[22, 26, 29] Furthermore, these thiol-ene hydrogels are susceptible to hydrolytic degradation due to the presence of an ester bond between the cyclic olefin and PEG backbone (Scheme 1). Here, we report the improved network crosslinking of thiol-ene hydrogels as compared to Michael-type addition hydrogels with similar macromer formulations. We also systematically study the hydrolytic degradation behaviors of thiol-ene hydrogels through experimental efforts and theoretical modeling. A statistical-co-kinetics model developed by Metters *et al.* for predicting hydrolytic degradation of step-growth Michael-type addition hydrogels was employed to predict the hydrolytic degradation of thiol-ene hydrogels due to their similarity in the degradation mechanism and the network structure.[13, 30]

Experimental Section

Materials

4-arm PEG−OH was purchased from JenKem Technology USA. Fmoc amino acids and coupling reagents for peptide synthesis were acquired from Anaspec. All other chemicals were obtained from Sigma-Aldrich unless noted otherwise.

Synthesis of PEG macromers and photoinitiator

Poly(ethylene glycol)-tetra-norbornene (PEG4NB) was synthesized using an established protocol.[22, 26] Briefly, norbornene anhydride was formed by reacting 5-norbornene-2-carboxylic acid (5-fold excess of −OH group on multi-arm PEG) and coupling reagent N,N′-dicyclohexylcarbodiimide (DCC, 2.5-fold excess of −OH group) in anhydrous dichloromethane (DCM) for 15 minutes at room temperature. The later was filtered through a fritted funnel into a second flask containing 4-arm PEG-OH (20 kDa), 4-(dimethylamino)pyridine (DMAP, 0.5-fold of −OH group), and pyridine (5-fold excess of −OH group) in DCM (kept in an ice bath). After overnight reaction, the product was washed with 5% sodium bicarbonate solution twice and brine once, followed by precipitation in cold ethyl ether. The product was then filtrated, re-dissolved in minimum amount of DCM, and re-precipitated in ether. Poly(ethylene glycol)-tetra-acrylate (PEG4A) was synthesized through reacting 4-arm PEG-OH (20 kDa) with acryloyl chloride (4-fold excess of −OH group) in the presence of triethylamine (TEA, 4.4-fold excess of −OH group) in toluene.[8, 31]

After overnight reaction, the solution was filtered through a thin layer of neutral aluminum oxide. Sodium carbonate was added to the solution and the heterogeneous solution was stirred for 2 hours in the dark. The solution was then filtered through Hyflo filtration aid and the clear solution obtained was precipitated in cold ether. High degree of PEG functionalization (>90 %) was confirmed by ^{1}H NMR (Bruker 500). The synthesis of photoinitiator lithium arylphosphonate (LAP) was performed as reported elsewhere.[32]

Microwave-assisted solid-phase peptide synthesis (SPPS)

All peptides were synthesized and cleaved in a microwave peptide synthesizer (CEM Discover SPS) following standard solid phase peptide synthesis procedure using Fmoc-protected amino acids. Cleaved peptides were precipitated in cold ether, dried in vacuo, purified by reverse phase HPLC (PerkinElmer Flexar system), and characterized with mass spectrometry (Agilent Technologies). The purity of the synthesized peptides was at least 90 %.

Hydrogel fabrication and swelling

Step-growth thiol-ene hydrogels were formed by radical-mediated photopolymerization between macromer PEG4NB and di-thiol containing crosslinkers, such as dithiothreitol (DTT) or cysteine-containing peptides (Scheme 1). Unless otherwise stated, a unity molar ratio between thiol and ene groups was used. Thiol-ene photopolymerization was initiated by 1 mM LAP under ultraviolet light exposure (365 nm, 5 mW/cm^2) in double distilled water (ddH_2O) or aqueous buffered solutions for 3 minutes. Step-growth Michael-type addition hydrogels were formed between PEG4A and DTT at pH 8.0. Step-growth Michael-type hydrogels were formed from PEG4A and DTT (at stoichiometric ratio) in a humidified oven (37 °C) overnight to ensure complete gelation.

For swelling studies, each gel was prepared from 50 μL precursor solution. After gelation, hydrogels were incubated in ddH_2O at 37 °C on an orbital shaker for 48 hours to remove uncrosslinked (sol fraction) species. Gels were then dried and weighed to obtain dried polymer weights (W_{Dry}). The dried polymers were then incubated in 5 mL of buffer solution (pH 6.0, pH 7.4 or pH 8.0 PBS) at 37 °C on an orbital shaker. At pre-determined time intervals, hydrogels were removed from the medium, blotted the gel surface with Kimwipe tissue, and weighed to obtained swollen weights ($W_{Swollen}$). Hydrogel mass swelling ratios (q) at equilibrium were defined as:

$$q=\frac{W_{Swollen}}{W_{Dry}} \quad (1)$$

As described by Metters et al.[6, 7], the mass swelling ratio (q) of a hydrolytically degrading network increases exponentially as a function of degradation time:

$$q=q_o e^{-k_{hyd}t} \quad (2)$$

Here, q_0 represents the initial mass swelling ratio before significant occurrence of degradation and k_{hyd} is the apparent pseudo first-order ester hydrolysis rate constant, which was obtained via exponential curve fitting to the experimental swelling data.

Rheometry

For rheometrical property measurements, hydrogel slabs were fabricated between two glass slides separated by 1 mm thick spacers. Circular gel discs (8 mm in diameter) were punched out from the gel slabs using a biopsy punch and placed in pH 7.4 PBS for 48 hours. Strain sweep (0.1 % to 20 %) oscillatory rheometry was performed on a Bohlin CVO 100 digital rheometer. Shear moduli of the hydrogels were measured using a parallel plate geometry (8 mm) with a gap size of 800 μm. Tests were performed in the linear viscoelastic region (LVR). *In situ* gelation rheometry for thiol-ene hydrogels was conducted in a UV cure cell at room temperature. Briefly, the macromer solution was placed on a quartz plate in the UV cure cell, and irradiated with UV light (Omnicure S1000, 365 nm, 5 mW/cm^2) through a liquid light guide. *In situ* gelation rheometry for Michael-type hydrogels was measured at 37°C using an 8 mm parallel plate geometry. Time sweep *in situ* rheometry was performed with 10 % strain, 1 Hz frequency, 0.1 N normal force, and a gap size of 100 μm. Gel point (i.e., crossover time) was determined at the time when storage modulus (G') surpassed loss modulus (G'').

Network structure of step-growth hydrogels

A perfectly crosslinked (or 'ideal') thiol-ene or Michael-type hydrogel network without defects can be estimated by means of hydrogel equilibrium swelling.[13] Considering the structural information of the step-growth hydrogels (i.e., macromer molecular weight and functionality), the average molecular weight between crosslinks ($\overline{M_c}$) is defined as:[13]

$$\overline{M_c}=2\left(\frac{MW_A}{f_A}+\frac{MW_B}{f_B}\right) \quad (3)$$

Here, MW_A and MW_B represent the molecular weight of PEG4NB (or PEG4A) and crosslinker, respectively. f_A and f_B are the number of reactive functionality for PEG4NB (or PEG4A) and crosslinker. With a known $\overline{M_c}$, the ideal network crosslinking density or density of elastically active chains (v_c) and polymer volume fraction (v_2) can be calculated based on the Flory-Rehner theory:[33, 34]

$$v_c=\frac{V_1}{\overline{M_c}\overline{v_2}}=\frac{-\left[ln\left(1-v_2\right)+v_2+^x{}_{12}{v_2}^2\right]}{{v_2}^{1/3}-\frac{2v_2}{f_A}} \quad (4)$$

Here, $\overline{v_2}$ is the specific volume of PEG (0.92 cm^3/g at 37 °C), V_1 is the molar volume of water (18 cm^3/mole) and χ_{12} is the Flory-Huggins interaction parameter for a PEG-H_2O system (0.45). After obtaining v_2, ideal hydrogel mass swelling ratio q can be obtained using the following equation:

$$v_2=\frac{\overline{v_2}}{\left(q-1\right)\overline{v_1}+\overline{v_2}} \quad (5)$$

where $\overline{v_1}$ is the specific volume of water (1.006 cm^3/g at 37 °C).

Prediction of hydrolytic degradation of thiol-ene hydrogels

A statistical-co-kinetic model established by Metters and Hubbell for predicting the hydrolytic degradation of step-growth hydrogels takes into account ester bond hydrolysis kinetics and the structural information such as the connectivity of the ideal hydrogel networks. Based on this model, the degradation of thiol-ene hydrogels was assumed to be purely due to ester bond hydrolysis with a pseudo-first order degradation kinetics.[6, 7] With this assumption, the fraction of hydrolyzed ester bonds (P_{Ester}) at any given time in the system is expressed as:

$$P_{Ester}=1-\frac{[Ester]}{[Ester]_0}=1-e^{-k't} \quad (6)$$

Here, *k'* is the pseudo-first order ester bond hydrolysis rate constant. [Ester] and $[Ester]_0$ are the current and initial numbers of intact ester bonds in the system.

The fraction of intact elastic chains (i.e., crosslinkers such as DTT or bis-cysteine containing peptides) within these crosslinked networks at any given time is expressed as:

$$1-P_{Chain}=(1-P_{Ester})^N=e^{-Nk't} \quad (7)$$

where N is the number of degradable units (i.e., ester bonds) connected to one elastic chain (e.g., N = 2 for the case of PEG4NB-DTT hydrogels).

To obtain the degree of crosslinking in the system, one must also consider the connectivity of multi-arm PEG macromers. For an ideal step-growth network, the fraction of f_A-armed macromer with *i* arms still connected to the network at any time point during ester hydrolysis is expressed as:[13]

$$F_{i,f_A}=\frac{f_A!}{\left(f_{A-i}\right)!i!}P_{chain}^{\left(f_{A-i}\right)}(1-P_{chain})^i \quad (8)$$

With this information, the crosslinking density of the degrading network is expressed as:

$$v_c=\left(\Sigma_{i=3}^{f_A}\frac{i}{2}F_{i,f_A}\right)[A]_0 \quad (9)$$

Here, $i \geq 3$ because any f_A-arm ($f_A \geq 3$) macromer with only two arms connected to intact elastic chains forms an extended loop, rather than a crosslink. $[A]_0$ represents the concentration of f_A-arm macromers (e.g., PEG4NB) in the equilibrium swelling state before the onset of network degradation, which is correlated to the crosslinking density of a network:

$$v_{c,0}=\frac{f_A}{f_B}[A]_0 \quad (10)$$

When the functionalities of the macromer and crosslinker (f_A = 4 and f_B = 2) are taken into account, the crosslinking density of a perfectly crosslinked thiol-ene network in the equilibrium state could be derived from Eqs. (4) to (10) and expressed as:

$$v_c=\left(6e^{-3NK't}-4e^{-4NK't}\right)[A]_{0,actual} \quad (11)$$

For gels with non-idealities, based on Eqs. (4), (5), and (11), $[A]_{0,actual}$ is obtained using actual crosslinking density as:

$$[A]_{0,actual}=\frac{v_{c,actual}}{v_{c,ideal}}[A]_0 \quad (12)$$

where $v_{c,actual}$ represents the experimental crosslinking density converted from experimental mass swelling ratio using Eqs. (4) and (5) and $v_{c,ideal}$ represent ideal crosslinking density calculated based on $\overline{M_c}$ derived from Eq. (3).

Enzymatic degradation study

4 wt% PEG4NB hydrogels (30 μL/gel) were crosslinked by bis-cysteine containing peptides with different percentages of chymotrypsin-sensitive (CGGY↓C: arrow indicates cleavage site) and non-sensitive (CGGGC) sequences. Hydrogels were fabricated using methodology described above and incubated in 500 μL PBS containing 0.5 mg/mL of chymotrypsin (Worthington Biochemical) at room temperature on an orbital shaker. At specific time points, hydrogels were removed from the chymotrypsin solution, blotted dry, measured the swollen mass, and placed back into the chymotrypsin solution. Fresh chymotrypsin solution was prepared every 15 minutes to ensure enzyme activity. Percent mass loss is defined as:

$$Mass\,loss\,(\%)=\frac{W_t-W_o}{W_o}\times 100\% \quad (13)$$

where W_t is the gel weight measured at specific time points and W_0 is the mass measured at equilibrium swelling (48 hours).

Data analysis

Data analysis and curve fitting were performed on Prism 5 software. The pseudo-first order rate constant (*k'*) was determined using Matlab 2010 built-in curve-fit tool function. A best-fit *k'* was determined based on Matlab built-in trust region algorithm with an R^2 value of 0.95 or greater. Unless otherwise noted, all experiments were conducted independently for three times and the results were reported as mean ± S.D.

Results and Discussion

Network crosslinking of thiol-ene and Michael-type hydrogels

The network ideality and hydrolytic degradation behaviors of step-growth thiol-ene hydrogels received little attention in previous reports. Given the attractive features offered by this new class of biomaterials, we were interested in characterizing and understanding these properties. In addition, while it has been suggested that thiol-ene photopolymerization produces hydrogels with higher degree of crosslinking when compared to Michael-type addition hydrogels, no direct experimental comparison has been made to verify this claim. Here, we prepared step-growth thiol-ene or Michael-type hydrogels using PEG4NB or PEG4A macromers. DTT was used as a hydrogel crosslinker for both systems. Since PEG4NB and PEG4A used in this study have the same molecular weight (MW_A = 20 kDa) and functionality (f_A = 4), hydrogels crosslinked by these macromers without any structural defect would have the same degree of crosslinking at identical macromer concentration. Therefore, variations in hydrogel physical properties (e.g., swelling, modulus, etc.) could be used to evaluate the network connectivity. We first characterized the gelation kinetics of these two step-growth hydrogel systems via *in situ* rheometry. As shown in Fig. 1, the gel point of thiol-ene photo-click reaction was ~230-fold faster than that of Michael-type addition reaction (3 ± 1 vs. 689 ± 18 seconds). While the time required to reach complete gelation for thiol-ene photo-click reaction was less than 3 minutes (Fig. 1a), it took almost 25 – 30 minutes for the Michael-type reaction to reach complete gelation (Fig. 1b). In addition, the final shear modulus (G') for thiol-ene hydrogels was 4.3-fold higher than that of Michael-type hydrogels (2030 ± 80 Pa vs. 470 ± 20 Pa), indicating improved network connectivity in thiol-ene hydrogels.[1, 35, 36]

We further compared these two gel systems using hydrogel equilibrium swelling and shear modulus, both of which are directly related to hydrogel crosslinking density.[36] Based on Eq. (3), the molecular weight between crosslinks ($\overline{M_c}$) of these two step-hydrogel systems without defect should be identical (neglecting growth the minor difference in the molecular weight of norbornene and acrylate moiety) and was calculated as 10,154 Da. Accordingly, the mass swelling ratio of a perfectly crosslinked step-growth hydrogel ($q_{eq,\ \mathrm{ideal}}$) was calculated as 9.6 using Eqs. (4) and (5) (Table 1 and dashed line in Fig. 2). Experimentally, however, we found that thiol-ene hydrogels, when compared to Michael-type gels at identical macromer compositions, had lower mass swelling ratio (28.5 ± 2.2 vs. 44.5 ± 3.8) and higher elastic modulus (~1 vs. ~0.2 kPa) at the equilibrium state. These experimental results confirmed a previous notion that radical-mediated thiol-ene reaction, when compared to Michael-type conjugation reaction, produce step-growth hydrogels with faster gelation kinetics, less structural defects, higher degree of crosslinking, and improved gel mechanical properties.[22]

Effect of macromer concentrations on thiol-ene hydrogel network crosslinking

As shown in Table 1, an 'ideal' step-growth network with a fixed macromer composition and without defect should only have a single equilibrium swelling ratio. Furthermore, the swelling ratio should be independent of macromer concentrations at equilibrium state. The experimental equilibrium mass swelling ratios of PEG4NB-DTT gels, however, exhibited

high dependency on PEG4NB macromer concentration as shown in Fig. 2. For example, when the concentration of PEG4NB macromer was increased from 4 wt% to 20 wt%, swelling ratios decreased from 28.5 ± 2.2 to 12.1 ± 0.2 and approached ideal equilibrium swelling ratio (9.6). Hydrogels with low swelling ratios (at higher macromer contents) had higher elastic moduli (~1 kPa and ~10 kPa for 4 wt% and 10 wt% PEG4NB-DTT hydrogels, respectively). This inverse relationship was commonly observed in chemically crosslinked networks, including chain-growth PEGDA hydrogels.

The trend observed in Fig. 2 could be attributed to a higher tendency of cyclization at lower PEG4NB contents. At diluted macromer concentrations, higher extent of intramolecular reactions led to formation of more primary cycles. Consequently, lower degree of intermolecular crosslinking resulted in increased gel swelling, and vice-versa.[13] The network defects resulting from different degrees of intramolecular and intermolecular reactions were the major reason for the dependency of experimental equilibrium swelling ratios on macromer concentrations.[13]

The strong dependency between macromer concentration (especially at lower concentrations) and network ideality in thiol-ene hydrogels was beneficial in that the physical properties (e.g., swelling and modulus) of these thiol-ene hydrogels could be easily tuned for biological applications (Fig. 2). For example, hydrogel shear moduli obtained (~1 to 10 kPa) using current thiol-ene hydrogel formulations were within a physiologically-relevant range and could be used to study the effect of matrix stiffness on cell fate processes.[37, 38] More importantly, the gelation time for these thiol-ene hydrogels was drastically shortened when compared to the crosslinking of chain-growth PEGDA or step-growth Michael-type hydrogels.

Effect of pH on degradation of PEG4NB-DTT hydrogels

As stated previously, thiol-ene hydrogels could be degraded hydrolytically via ester hydrolysis. We found that the degradation of thiol-ene hydrogels was pH-dependent (Fig. 3). PEG4NB-DTT hydrogels incubated in acidic condition (pH 6.0) were stable with an almost constant swelling ratio over a 45-day period, whereas hydrogels with the same compositions exhibited increasing swelling over time in slightly basic conditions (pH 7.4 and pH 8.0). We conducted exponential curve fittings using the swelling data of degrading hydrogels and found high degree of correlation between the fitted curves with the experimental data (dashed curves, $R^2 = 0.98$ for both pH 7.4 and pH 8.0 in Fig. 3), indicating that the degradation of thiol-ene hydrogels was most likely a result of pseudo-first order ester bond hydrolysis.

Since the two basic pH conditions yielded significantly different degradation rates (Table 2), we were interested to know if gel degradation in different pH values assumed the same degradation mechanism. A previous study concerning the degradation of thiol-acrylate photopolymer networks revealed that, if the degradation follows the same ester hydrolysis mechanism at an elevated pH value (e.g., from pH 7.4 to pH 8.0), the two degradation profiles could be described using a pseudo-first order equation:[17]

$$[Ester] = [Ester]_0 e^{-k'[OH^-]t} \quad (14)$$

In the above equation, the influence of hydroxyl ion concentration was separated from the pseudo-first order kinetic constant since pH was no longer a constant in the experimental setting. If the network degradation was purely due to ester bond hydrolysis in different pH values, the degradation could still be described using the same ester hydrolysis rate constant (*k'*) if a factor of 4 was multiplied to the degradation time. In another word, the two degradation curves (at pH 7.4 and pH 8.0) would overlap after adjusting the degradation time to account for the 4-fold increase in the OH^- ion concentrations between the two pH values.[17] Similarly, the factor of 4 could be incorporated into *k'* to reflect the accelerated degradation kinetics. Consequently, one would expect to obtain a 4-fold increase in the ratio of the apparent degradation rate constants (k_{hyd}) for hydrogels degraded in the two pH values. However, the exponential curve fitting performed in Fig. 3 (k_{hyd} = 0.057 ± 0.002 and 0.024 ± 0.001 day^{-1} pH 8.0 and pH 7.4, respectively) yielded a k_{hyd} ratio of 2.4, rather than the ideal 4-fold increase (Table 2). This significantly lowered k_{hyd} ratio suggested that the degradation was not solely governed by simple ester bond hydrolysis and other factors could also play a role on the degradation rate of these thiol-ene hydrogels.

In addition to the experimental work, we also utilized a statistical-co-kinetic model to predict the hydrolytic degradation of thiol-ene hydrogels. Using this model (Eq. (11)), we chose a best-fit *k'* of 0.011 day^{-1} (R^2 = 0.96) and 0.027 day^{-1} (R^2 = 0.95) for the degradation of 4 wt% PEG4NB-DTT hydrogels in pH 7.4 and pH 8.0, respectively (Table 2). Note that these *k'* values were selected only to validate the model predictions at different degradation conditions, and by no means to suggest any 'ideality' in the crosslinked network since the gels at these conditions were not 'ideal' as discussed in the previous sections. As stated above, if the thiol-ene network degradation was governed solely by ester bond hydrolysis, a *k'* of 0.044 day^{-1} (4-fold of $k'_{pH7.4}$ = 0.011 day^{-1}) could be used to predict gel degradation occurred at pH 8.0. However, the best-fit *k'* was 0.027 day^{-1} (R^2 = 0.95) for degradation occurred at pH 8.0, which only yielded a ratio of 2.5 (compared to $k'_{pH7.4}$ = 0.011 day^{-1}), and again was much slower than the theoretical 4-fold difference (Table 2). A potential explanation for this phenomenon is base-catalyzed oxidation of thioether bond forming between norbornene and thiol groups (Scheme 1), which was likely promoted at higher pH values[39] and influenced the rate of ester hydrolysis. Another possible reason for the lower-than-predicted degradation rate at higher pH values was that the degradation process produced acidic by-products (Scheme 1), which decreased acidity and retarded the degradation. Further investigations, however, are required to elucidate the exact mechanisms.

Effect of macromer concentration on degradation of PEG4NB-DTT hydrogels

We further evaluated the hydrolytic degradation of PEG4NB-DTT hydrogels with different macromer concentrations (4 and 10 wt%) in pH 7.4 (Fig. 4a) and pH 8.0 (Fig. 4b). We observed experimentally that hydrogels prepared from a precursor solution containing lower weight content of PEG4NB (e.g., 4 wt%) degraded at a slightly faster rate (e.g., 0.024 ±

0.001 and 0.020 ± 0.001 day^{-1} for 4 wt% and 10 wt% PEG4NB at pH 7.4, respectively. Table 2), regardless of pH value. Model prediction also followed the same trend where higher best-fit k' values were obtained for gels made from lower PEG4NB concentration (e.g., 0.011 and 0.009 day^{-1} for 4 wt% and 10 wt% PEG4NB at pH 7.4, respectively. Table 2). This study suggested that the effect of macromer concentration affected not only the initial network crosslinking (i.e., network ideality), but also the rate of network hydrolytic degradation.

Effect of initial crosslinking density on degradation of PEG4NB-DTT hydrogels

Results in Fig. 4 revealed that the degradation rate of thiol-ene hydrogels could be affected by the degree of initial network crosslinking, a characteristic different from Michael-type addition hydrogels. In order to further validate this observation, we conducted additional studies using both theoretical and experimental approaches. We first predicted, using Eq. (11), the degradation profiles of ideal thiol-ene hydrogels with different degrees of crosslinking by varying the stoichiometric ratios of thiol to ene moieties (i.e., $R_{[thiol]/[ene]}$ = 0.6, 0.8, and 1). This parametric manipulation yielded hydrogels with different initial crosslinking densities ($[A]_{0,\ ideal}$ = 5.78 × 10^{-4}, 7.71 10^{-4},and 9.63 × × 10^{-4} M for $R_{[thiol]/[ene]}$ = 0.6, 0.8, and 1, respectively). In these predictions, a fixed hydrolysis rate constant (*k'* = 0.063 day^{-1}) was selected based on a value reported for the degradation of step-growth Michael-type hydrogels.[30] As shown in Fig. 5, the ideal initial mass swelling ratio at different degree of network crosslinking ($R_{[thiol]/[ene]}$ = 0.6, 0.8 and 1) varied only slightly between 9.6 and 11.9. Since the assumption in this prediction was that the rate of degradation is independent of the initial degree of network crosslinking, a single *k'* yielded three degradation profiles with only slight variation.

To validate the prediction shown in Fig. 5, we designed thiol-ene hydrogels with different initial degree of crosslinking by altering the concentrations of crosslinker used (DTT, $R_{[thiol]/[ene]}$ = 0.6, 0.8 and 1) while keeping a constant PEG4NB macromer content (4 wt%) during gelation. As expected, decreasing initial network crosslinking (e.g., $R_{[thiol]/[ene]}$ = 0.6) resulted in a significant increase in initial hydrogel swelling (*q* = 69.2 ± 3.0) due to increased network non-ideality (Fig. 6a). This phenomenon was similar to the results shown in Fig. 2 where hydrogels prepared from lower PEG4NB weight contents had significantly higher initial swelling. When the difference in the initial degree of swelling was taken in to account in the model prediction, one would expect similar degradation trends as shown in Fig. 5 where the profiles could be predicted using a single *k'*. Interestingly, our experimental results showed that thiol-ene network crosslinked with low $R_{[thiol]/[ene]}$ exhibited not only very high equilibrium swelling ratios, but also much faster degradation rates (Table 3). When the degradation profiles were fitted with Eq. (11), the best-fit *k'* values were 0.035, 0.017, and 0.011 day^{-1} for $R_{[thiol]/[ene]}$ = 0.6, 0.8, and 1, respectively (Table 3). In another word, the degradation rate constants were accelerated (2- to 3-fold) as a function of network non-ideality. The accelerated gel degradation was confirmed via rheometrical measurements where gels reached complete disintegration by day 21 and day 28 for $R_{[thiol]/[ene]}$ = 0.6 and 0.8, respectively (Fig. 6b). Based on this discussion, the higher network non-ideality of Michael-type gels is likely the major reason for faster degradation rate as reported in literature when compared to the thiol-ene hydrogels.**(a) (b)**

Results shown in Figs. 4 and 6 were different from previous reports for hydrolytic degradation of Michael-type hydrogels. For example, the prediction and verification results from Metters *et al.* showed that a single *k'* could be used to describe the degradation occurred at different initial crosslinking densities, indicating the hydrolysis of thioether-ester bonds forming between PEG-acrylate and DTT was not affected by factors other than simple hydrolysis (e.g., macromer concentration, crosslinking efficiency, etc.).[13] In fact, previous models developed for predicting the hydrolysis of PEG hydrogels were based on the assumptions that the factors affecting hydrolysis could be 'lumped' into a pseudo-first order hydrolysis rate constant or *k'*.[5-7, 13] These factors include water or hydronium ion concentrations, temperature, pH values, etc. For highly swollen hydrogels ($q > 10$), these factors are often negligible at constant temperature and pH value, thus the degradation profiles of the hydrogels could be predicted using the same *k'* regardless of macromer composition or degree of network crosslinking. While the degradation of thiol-ene hydrogels was mediated by ester bond hydrolysis, our data suggested that it was also affected by other environmental and/or structural factors (such as densities of cyclic olefin groups and thioether bonds at different macromer contents). The mechanisms or factors affecting the hydrolytic degradation rate of thiol-ene hydrogels at different initial crosslinking densities are yet to be determined. Nonetheless, a general trend observed from our studies was that thiol-ene hydrogels with higher degree of crosslinking degraded at a slower rate than gels with lower degree of crosslinking.

Effect of crosslinker sequence on network properties of PEG4NB-peptide hydrogels

In previous sections, we have learned that there was a high inter-dependency between the degree of thiol-ene hydrogel network crosslinking and the subsequent degradation rates using DTT as a hydrogel crosslinker. Recent studies have shown that PEG hydrogels crosslinked by peptide crosslinkers are useful in creating biomimetic extracellular microenvironments.[12, 26] Here, we investigated the influence of peptide sequences on the crosslinking and degradation of step-growth thiol-ene hydrogels. As a model system to illustrate the importance of peptide sequences on thiol-ene hydrogel degradation, we synthesized three simple peptide crosslinkers with only one amino acid variation: CGGGC, CGGYC and CGGLC. The molecular weights of these three peptide crosslinkers (MW_B) varied slightly between 394 to 501 Da (Table 4), which would only cause minimum influence in the chain length between adjacent crosslinks due to the relatively large PEG4NB macromolecules (MW_A = 20 kDa) used.

Table 4 shows the physical properties of 4 wt% PEG4NB-peptide hydrogels crosslinked by peptide crosslinker with different sequences. These PEG4NB-peptide hydrogels all had rapid gel points (~4 to 5 seconds), which were consistent with our previous studies in thiol-ene hydrogels.[24] Similar to the degradation of PEG4NB-DTT gels shown in Figs. 4 and 6, PEG-peptide hydrogel degradation rates were affected by the initial degree of network crosslinking. As shown in Fig. 7, peptide sequences affected both initial crosslinking as well as subsequent hydrolytic degradation rate. At the same macromer weight content (4 wt%), the initial swelling ratios of PEG4NB-peptide hydrogels were significantly higher than that of PEG4NB-DTT hydrogels. As a result, these PEG4NB-peptide hydrogels exhibited faster hydrolytic degradation rates (Table 4). Interestingly, hydrogels crosslinked by CGGGC and

CGGYC peptides had similar initial swelling (Fig. 7a), but the degradation rate constant was significantly lower for gels crosslinked by CGGYC (~26% lower in k_{hyd}; ~30% lower in k'. Table 4). Furthermore, hydrogels crosslinked by peptides containing aromatic (e.g., CGGYC) or hydrophobic (e.g., CGGLC) residues yielded slower degradation rates compared to gels crosslinked by simple CGGGC linker, potentially due to steric hindrance and hydrophobic effect of tyrosine and leucine residues that retarded degradation (Table 4). As expected, the swelling of these PEG4NB-peptide hydrogels was inversely correlated to the elastic moduli (Fig. 7b). Hydrogels crosslinked by CGGGC peptide degraded completely in about 15 days (modulus dropped from ~1.0 kPa to ~0.1 kPa from day 0 to day 14), while gels crosslinked with CGGYC or CGGLC lasted at least 21 days until complete gel disintegration. This study revealed that the degradation of thiol-ene hydrogels could be easily tuned by altering identity of the peptide crosslinkers.

Effect of protease sensitivity on thiol-ene hydrogel degradation

Many step-growth hydrogels have been prepared for protease-sensitive degradation by incorporating peptidyl substrates as hydrogel crosslinkers.[12, 24, 26, 29, 40-44] Here, we sought to combine enzymatic and hydrolytic degradation properties of thiol-ene hydrogels and create dual-mode degradable hydrogels without altering hydrogel molecular structure or hydrophilicity. By combining peptide crosslinkers with different protease sensitivities, we found that the degradation behaviors of thiol-ene hydrogels could be easily manipulated and changed from completely surface erosion to bulk degradation. Here, hydrogels were crosslinked by 4 wt% PEG4NB and stoichiometric ratio of non-cleavable CGGGC and/or chymotrypsin cleavable CGGY↓C peptides at various compositions (percent molar ratio of CGGYC:CGGGC = 100:0, 75:25, 50:50, 25:75 and 0:100, Fig. 8). Note that the overall molar ratio of thiol to ene moieties was stoichiometric balanced for all conditions ($R_{[ene]/[thiol]} = 1$). When these gels were exposed to chymotrypsin solution, hydrogels containing high percentage of CGGYC crosslinker (100% to 75%) eroded rapidly by surface erosion, evidenced by linearly increasing mass loss profiles with time. These gels reached complete erosion at around 10 and 16 minutes for gels incorporated with 100% and 75% of CGGYC, respectively (Fig. 8). Interestingly, when the total content of CGGYC peptide was decreased to 50% and 25%, chymotrypsin treatment led to increased gel mass (i.e., negative mass loss). These gels continued to swell and gained mass for the remaining course of study, indicating that protease treatment led to a 'loosened' gel structure and increased water uptake. The degradation mode was likely transitioned from a surface erosion to a bulk degradation mechanism. On the other hand, chymotrypsin treatment had no effect on the swelling or mass loss of thiol-ene hydrogels crosslinked by non-chymotrypsin sensitive linker (CGGGC). These results suggested that by altering protease sensitivity of PEG4NB-peptide hydrogels through elegant selection of peptide crosslinkers, the mode of degradation profiles could also be manipulated and may be used to dynamically control growth factor delivery in the future.

Conclusions

In summary, we showed that PEG hydrogels formed by step-growth thiol-ene photopolymerizations exhibited high degree of tunability in network crosslinking and

degradation. In addition to the improved network properties compared to Michael-type hydrogels, we also found that thiol-ene hydrogels were hydrolytically degradable and the degradation was base-catalyzed and followed a bulk degradation mechanism. Through experimental and theoretical investigations, we found that the degradation of thiol-ene hydrogels was primarily governed by ester bond hydrolysis and was accelerated as network non-ideality increases. In addition, we were able to tune and predict the hydrolytic degradation behavior of thiol-ene hydrogels by manipulating the degree of network crosslinking and crosslinking peptide sequences. By altering thiol-ene hydrogel protease sensitivity, the mode of thiol-ene hydrogels degradation could be switched between surface erosion and bulk degradation. These studies provide further understanding on the network properties of the thiol-ene hydrogels, which should benefit the utilization of this diverse hydrogel system in tissue engineering applications.

Acknowledgments

This project was funded by the Department of Biomedical Engineering at IUPUI, a Research Support Funds Grant (RSFG) from IUPUI Office of the Vice Chancellor for Research (OVCR), and NIH/NIBIB (R21EB013717). The authors thank Mr. Asad Raza for his assistance on PEG4NB synthesis.

Reference

1. Anseth KS, Metters AT, Bryant SJ, Martens PJ, Elisseeff JH, Bowman CN. Journal of Controlled Release. 2002; 78:199–209. [PubMed: 11772461]
2. Bryant SJ, Anseth KS. Journal of Biomedical Materials Research. 2002; 59:63–72. [PubMed: 11745538]
3. Peppas NA, Hilt JZ, Khademhosseini A, Langer R. Advanced Materials. 2006; 18:1345–1360.
4. Lin CC, Anseth KS. Pharmaceutical Research. 2009; 26:631–643. [PubMed: 19089601]
5. Metters AT, Anseth KS, Bowman CN. Polymer. 2000; 41:3993–4004.
6. Metters AT, Bowman CN, Anseth KS. Journal of Physical Chemistry B. 2000; 104:7043–7049.
7. Metters AT, Anseth KS, Bowman CN. Journal of Physical Chemistry B. 2001; 105:8069–8076.
8. Sawhney AS, Pathak CP, Hubbell JA. Macromolecules. 1993; 26:581–587.
9. He S, Timmer MD, Yaszemski MJ, Yasko AW, Engel PS, Mikos AG. Polymer. 2001; 42:1251–1260.
10. Cho E, Kutty JK, Datar K, Lee JS, Vyavahare NR, Webb K. Journal of Biomedical Materials Research Part A. 2009; 90A:1073–1082. [PubMed: 18671270]
11. Elbert DL, Pratt AB, Lutolf MP, Halstenberg S, Hubbell JA. Journal of Controlled Release. 2001; 76:11–25. [PubMed: 11532309]
12. Lutolf MP, Lauer-Fields JL, Schmoekel HG, Metters AT, Weber FE, Fields GB, Hubbell JA. Proceedings of the National Academy of Sciences of the United States of America. 2003; 100:5413–5418. [PubMed: 12686696]
13. Metters A, Hubbell J. Biomacromolecules. 2005; 6:290–301. [PubMed: 15638532]
14. van de Wetering P, Metters AT, Schoenmakers RG, Hubbell JA. Journal of Controlled Release. 2005; 102:619–627. [PubMed: 15681084]
15. Rydholm AE, Bowman CN, Anseth KS. Biomaterials. 2005; 26:4495–4506. [PubMed: 15722118]
16. Rydholm AE, Reddy SK, Anseth KS, Bowman CN. Biomacromolecules. 2006; 7:2827–2836. [PubMed: 17025359]
17. Rydholm AE, Anseth KS, Bowman CN. Acta Biomaterialia. 2007; 3:449–455. [PubMed: 17276150]
18. Rydholm AE, Reddy SK, Anseth KS, Bowman CN. Polymer. 2007; 48:4589–4600. [PubMed: 18626514]

19. Zustiak SP, Leach JB. Biomacromolecules. 2010; 11:1348–1357. [PubMed: 20355705]
20. Zustiak SP, Leach JB. Biotechnology and Bioengineering. 2011; 108:197–206. [PubMed: 20803477]
21. Lin-Gibson S, Jones RL, Washburn NR, Horkay F. Macromolecules. 2005; 38:2897–2902.
22. Fairbanks BD, Schwartz MP, Halevi AE, Nuttelman CR, Bowman CN, Anseth KS. Advanced Materials. 2009; 21:5005–5010.
23. Hoyle CE, Bowman CN. Angewandte Chemie-International Edition. 2010; 49:1540–1573.
24. Lin CC, Raza A, Shih H. Biomaterials. 2011; 32:9685–9695. [PubMed: 21924490]
25. Fairbanks BD, Singh SP, Bowman CN, Anseth KS. Macromolecules. 2011; 44:2444–2450. [PubMed: 21512614]
26. Anderson SB, Lin CC, Kuntzler DV, Anseth KS. Biomaterials. 2011; 32:3564–3574. [PubMed: 21334063]
27. Schwartz MP, Fairbanks BD, Rogers RE, Rangarajan R, Zaman MH, Anseth KS. Integrative Biology. 2010; 2:32–40. [PubMed: 20473410]
28. Benton JA, Fairbanks BD, Anseth KS. Biomaterials. 2009; 30:6593–6603. [PubMed: 19747725]
29. Aimetti AA, Machen AJ, Anseth KS. Biomaterials. 2009; 30:6048–6054. [PubMed: 19674784]
30. DuBose JW, Cutshall C, Metters AT. Journal of Biomedical Materials Research Part A. 2005; 74A:104–116. [PubMed: 15940664]
31. Lin CC, Metters AT. Pharmaceutical Research. 2006; 23:614–622. [PubMed: 16397740]
32. Fairbanks BD, Schwartz MP, Bowman CN, Anseth KS. Biomaterials. 2009; 30:6702–6707. [PubMed: 19783300]
33. Flory, P. Principles in Polymer Chemistry. Cornell University Press; Ithaca, NY: 1953.
34. Lin CC, Metters AT. Advanced Drug Delivery Reviews. 2006; 58:1379–1408. [PubMed: 17081649]
35. Anseth KS, Bowman CN, Peppas NA. Journal of Polymer Science Part a-Polymer Chemistry. 1994; 32:139–147.
36. Anseth KS, Bowman CN, BrannonPeppas L. Biomaterials. 1996; 17:1647–1657. [PubMed: 8866026]
37. Kloxin AM, Benton JA, Anseth KS. Biomaterials. 2010; 31:1–8. [PubMed: 19788947]
38. Kloxin AM, Kloxin CJ, Bowman CN, Anseth KS. Advanced Materials. 2010; 22:3484–3494. [PubMed: 20473984]
39. Napoli A, Valentini M, Tirelli N, Muller M, Hubbell JA. Nature Materials. 2004; 3:183–189.
40. Kraehenbuehl TP, Ferreira LS, Zammaretti P, Hubbell JA, Langer R. Biomaterials. 2009; 30:4318–4324. [PubMed: 19500842]
41. Kraehenbuehl TP, Zammaretti P, Van der Vlies AJ, Schoenmakers RG, Lutolf MP, Jaconi ME, Hubbell JA. Biomaterials. 2008; 29:2757–2766. [PubMed: 18396331]
42. Miller JS, Shen CJ, Legant WR, Baranski JD, Blakely BL, Chen CS. Biomaterials. 2010; 31:3736–3743. [PubMed: 20138664]
43. Patterson J, Hubbell JA. Biomaterials. 2010; 31:7836–7845. [PubMed: 20667588]
44. Tsurkan MV, Chwalek K, Levental KR, Freudenberg U, Werner C. Macromolecular Rapid Communications. 2010; 31:1529–1533. [PubMed: 21567562]

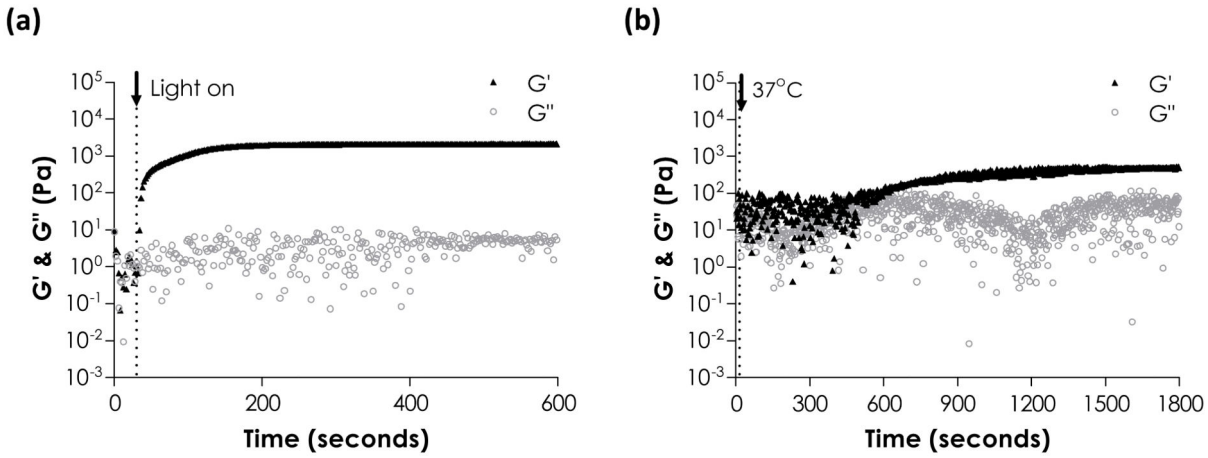

Figure 1.

In situ rheometry of step-growth hydrogels: (a) Thiol-ene photo-click polymerization (4 wt % PEG4NB-DTT). UV light was turned on at 30 seconds. (b) Michael-type addition (4 wt% PEG4A-DTT). Temperature reached 37 °C at 15 seconds.

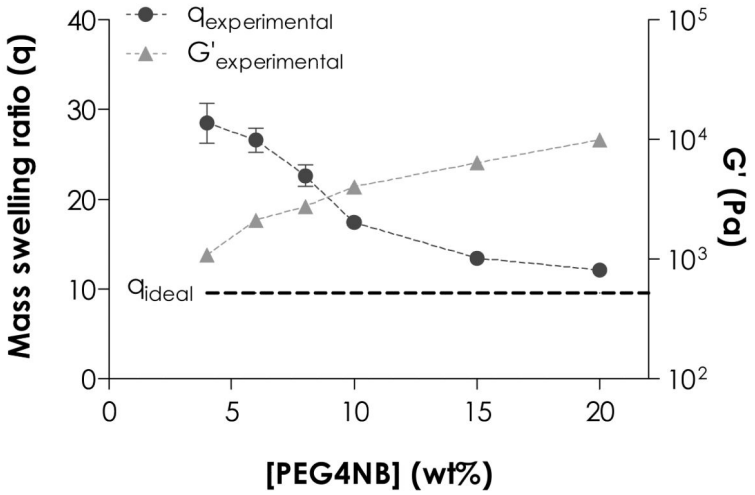

Figure 2.

Effect of PEG4NB macromer concentration on hydrogel equilibrium swelling (left y-axis) and elastic modulus (right y-axis). Swelling ratio of an ideal network was calculated based on the molecular weight between crosslinks ($\overline{M_c}$) of given macromer molecular weights (MW_{PEG4NB} = 20 kDa, MW_{DTT} = 154 Da) and functionalities f_{PEG4NB} = 4, f_{DTT} = 2).

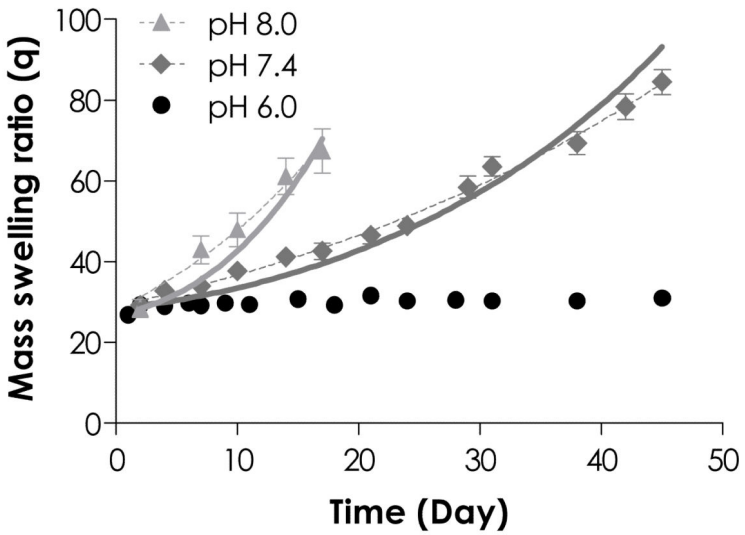

Figure 3.

Effect of buffer pH on mass swelling ratio of 4 wt% PEG4NB-DTT hydrogels. Symbols represent experimental data while dashed curves represent exponential curve fitting to the experimental data. The apparent degradation rate constants (k_{hyd}) for gels degraded in pH 7.4 and pH 8.0 were 0.024 ± 0.001 and 0.057 ± 0.002 day^{-1}, respectively. Solid curves represent model predictions with best-fit kinetic rate constants: $k'_{\text{pH 7.4}}$ = 0.011 day^{-1} and $k'_{\text{pH 8.0}}$ = 0.027 day^{-1}. No curve fitting or model prediction was made for gels degraded in pH 6.0 due to the stability of gels in acidic conditions.

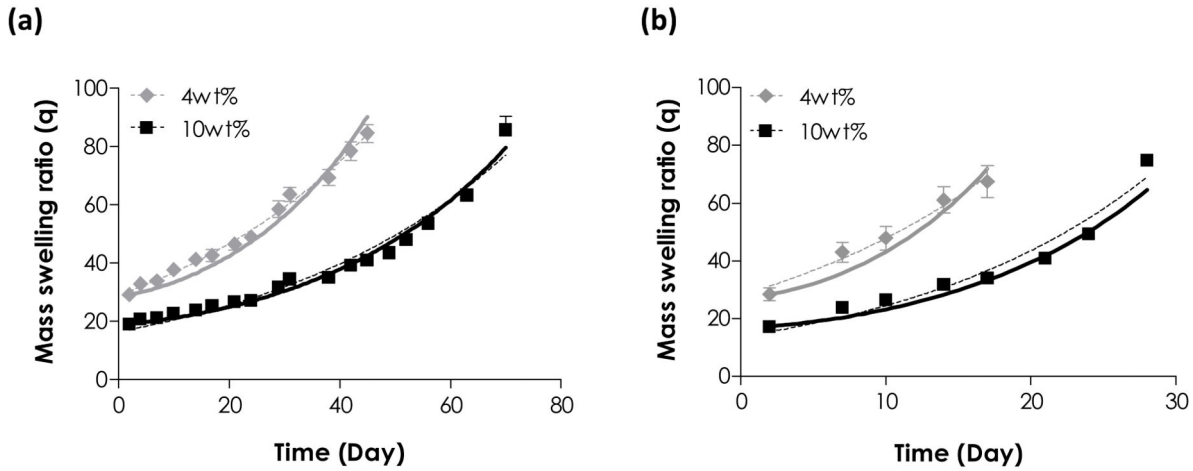

Figure 4.

Hydrolytic degradation of PEG4NB-DTT hydrogels with different macromer concentrations in (a) pH 7.4 and (b) pH 8.0 PBS. Symbols represent experimental data, dashed curves represent exponential fit, and solid curves represent model prediction (See Table 2 for hydrolysis rate constants selected).

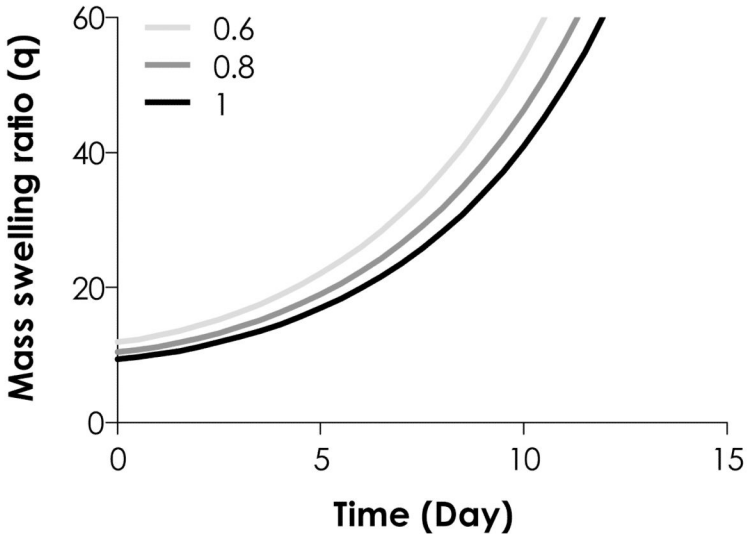

Figure 5.

Model prediction of thiol-ene hydrogel degradation starting from different initial crosslinking ($R_{[thiol]/[ene]}$ = 0.6, 0.8 and 1; k' = 0.063 day^{-1}).

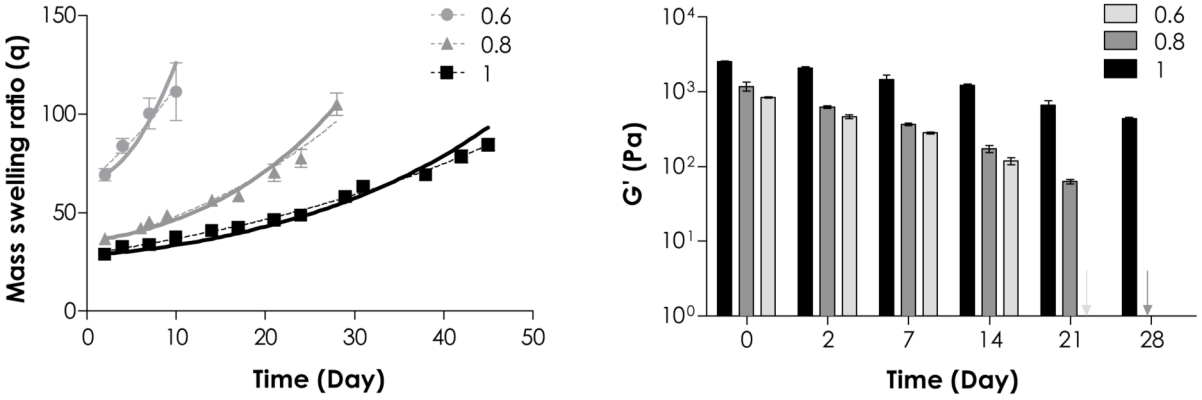

Figure 6.

Effect of initial network crosslinking on PEG4NB-DTT hydrolytic degradation. (a) Mass swelling ratio and (b) elastic moduli of 4 wt% PEG4NB-DTT hydrogels with $R_{[thiol]/[ene]}$ = 0.6, 0.8, and 1. Symbols represent experimental data, dashed curves represent exponential fit, and solid curves represent model prediction (See Table 3 for degradation rate constants selected).

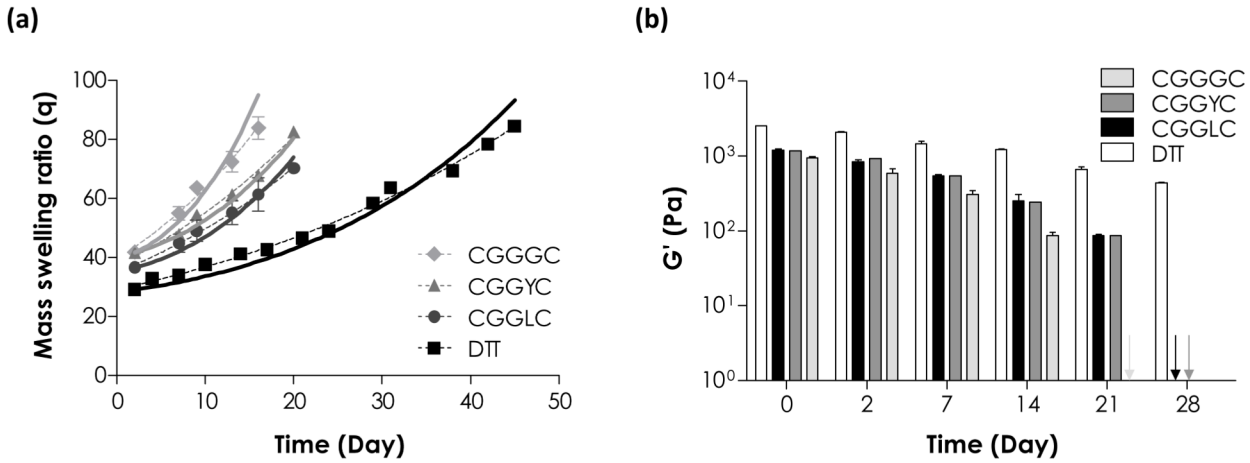

Figure 7.

Effect of crosslinker peptide sequences on PEG4NB-peptide hydrogels degradation. (a) Mass swelling ratio and (b) elastic modulus of PEG4NB hydrogels crosslinked by CGGGC, CGGYC or CGGLC peptides. PEG4NB-DTT hydrogels were used for comparison. Symbols represent experimental data, dashed curves represent exponential curve fits, and solid curves represent statistical-co-kinetics model fits to the experimental data. (4 wt% PEG4NB-peptide hydrogels, pH 7.4, N = 4)

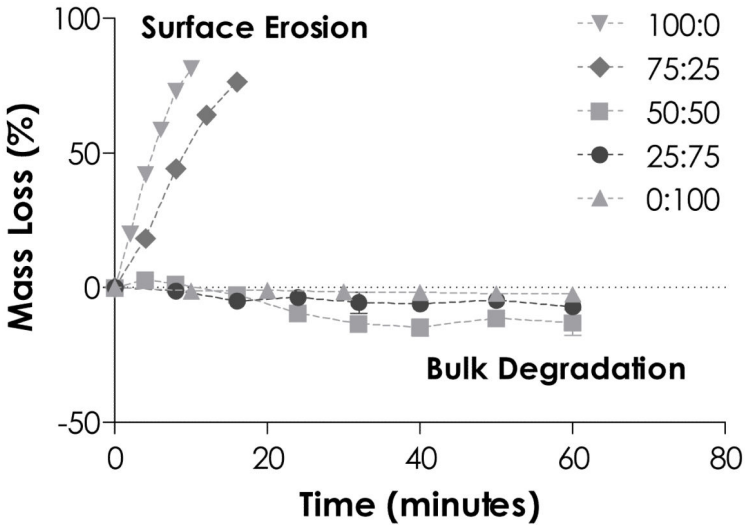

Figure 8.

Effect of peptide crosslinkers on PEG4NB-peptide hydrogels erosion/degradation. PEG4NB hydrogels crosslinked by different percentage of chymotrypsin sensitive (CGGYC) and non-degradable (CGGGC) peptides. Figure legends indicate the percent molar ratio of CGGYC:CGGGC. (4 wt% PEG4NB-peptide hydrogels, pH 7.4, N = 4)

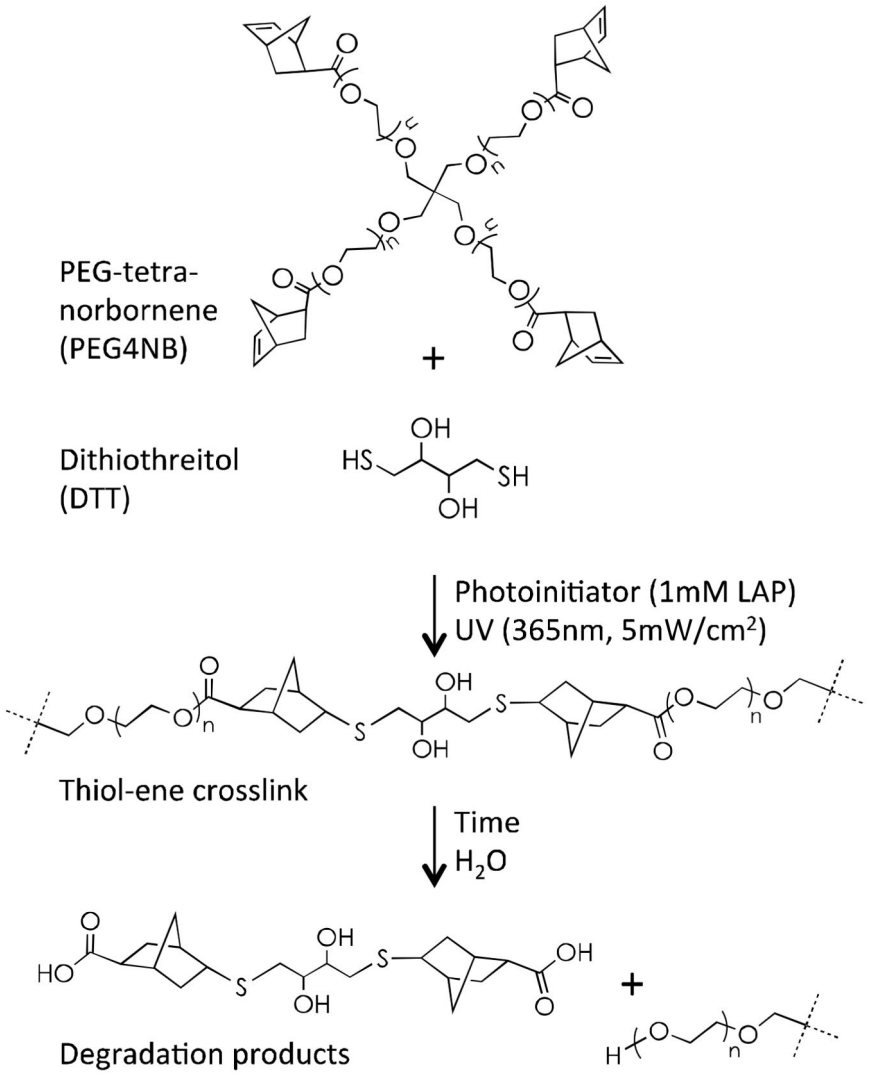

Scheme 1.

Schematics of photopolymerization and hydrolytic degradation of step-growth thiol-ene hydrogels. PEG-tetra-norbornene (PEG4NB) reacts with a bi-functional crosslinker DTT (dithiothreitol), in a step-growth manner, to form thioether linkage and crosslinked hydrogels. Hydrolytic degradation of the network occurs due to ester bond hydrolysis.

Table 1

Characteristics of step-growth Michael-type and thiol-ene hydrogels (4 wt%, 20 kDa, 4-arm PEG-derivatives crosslinked by DTT, pH 7.4, N = 4).

	$\overline{M_c}$ (g/mole)	$q_{eq,\ ideal}$	$q_{eq,\ actual}$	$G'_{eq,\ actual}$(kPa)
PEG4A (Michael-type)	10,154	9.6	44.5 ± 3.8	0.2 ± 0.01
PEG4NB (Thiol-ene)	10,154	9.6	28.5 ± 2.2	1.1 ± 0.1

Table 2

Hydrolytic degradation rate constants for PEG4NB-DTT hydrogel network. k_{hyd} and k' were obtained from exponential fit and statistical-co-kinetic model fit to the swelling data, respectively. (pH 7.4, N = 4)

[PEG4NB] (wt%)	PH	k_{hyd} (day^{-1})	R^2_{khyd}	Ratio of $k_{hyd,\ pH\ 8.0}/k_{hyd,\ pH\ 7.4}$	k' (day^{-1})	$R^2_{k'}$	Ratio of $k'_{pH\ 8.0}/k'_{pH\ 7.4}$
4	7.4	0.024 ± 0.001	0.98	2.4	0.011	0.96	2.5
	8.0	0.057 ± 0.002	0.98		0.027	0.98	
10	7.4	0.020 ± 0.001	0.98	2.5	0.009	0.95	2.3
	8.0	0.050 ± 0.001	0.99		0.021	0.96	

Table 3

Hydrolytic degradation rate constants for PEG4NB-DTT hydrogel network with different stoichiometric ratios. k_{hyd} and k' were obtained from exponential fit and statistical-co-kinetic model fit to the swelling data, respectively.

$R_{[thiol]/[ene]}$	$[A]_{o,\ ideal}$ (M)	k_{hyd} (day^{-1})	R^2_{khyd}	k' (day^{-1})	$R^2_{k'}$
0.6	5.78×10^{-4}	0.073 ± 0.002	0.96	0.035	0.95
0.8	7.71×10^{-4}	0.035 ± 0.004	0.97	0.017	0.96
1	9.63×10^{-4}	0.024 ± 0.001	0.98	0.011	0.96

Table 4

Parameters for PEG4NB-peptide hydrogel network. k_{hyd} and k' were obtained from exponential fit and statistical-co-kinetic model fit to the swelling data, respectively. (pH 7.4, N = 4)

Peptide Crosslinker	MW_B (Da)	Gel Point (sec)	k_{hyd} (day^{-1})	R^2_{khyd}	k' (day^{-1})	$R^2_{k'}$
CGGGC	394	5.3 ± 0.1	0.049 ± 0.001	0.98	0.026	0.96
CGGYC	501	4.5 ± 0.5	0.036 ± 0.004	0.99	0.018	0.98
CGGLC	451	4.3 ± 1.4	0.036 ± 0.002	0.99	0.017	0.98